ISSN 1063-7729, Astronomy Reports, 2021, Vol. 65, No. 3, pp. 209–223. © Pleiades Publishing, Ltd., 2021.
Russian Text © The Author(s), 2021, published in Astronomicheskii Zhurnal, 2021, Vol. 98, No. 3, pp. 239–254.

Improving the Orbits of Four Visual Binaries Using Gaia DR2 Data and Observations with the 26-inch Refractor of Pulkovo Observatory

L. G. Romanenko[a], * and I. S. Izmailov[a]

[a] *Main (Pulkovo) Astronomical Observatory, Russian Academy of Sciences, St. Petersburg, 196140 Russia*
**e-mail: lrom1962@list.ru*

Received December 19, 2019; revised September 28, 2020; accepted October 30, 2020

Abstract—We use a modified method of the apparent motion parameters (AMP), in which the initial data from the Gaia DR2 catalog are not only high-precision coordinates, parallaxes, and radial velocities of the components of the studied wide binary stars, but are also their proper motions. The coincidence of the AMP orbits obtained both from the Gaia DR2 data and from the Pulkovo series from 1960–2019 leads to an orbit that is unambiguous in terms of an ascending node. The results for improving the orbits of such visual binaries of the Pulkovo research program as ADS 246, 2757, 10386, and 12169 are presented. Orbits (with periods of 1226, 1075, 4500, and 4900 years), orbital orientation parameters in the Galaxy coordinate frame, and the masses of these systems are obtained (0.59 ± 0.05, 1.7 ± 0.3, 1.7 ± 0.4, and $2.25 \pm 0.5 M_{\odot}$). It is shown that dense homogeneous series of ground-based observations, such as CCD observations with the 26-inch refractor of the Pulkovo Observatory, do not lose their relevance, serve as the basis for identifying the best solution based on both Gaia data and our own observations, and should be continued. It was also shown that the Thiele–Innes method is not suitable for determining the orbits of binary stars with a separation of more than 100 AU. The paper is based on a presentation made at the conference "Astrometry yesterday, today, and tomorrow," which took place on October 14–16, 2019 at the Sternberg Astronomical Institute of Moscow State University.

DOI: 10.1134/S1063772921030021

1. INTRODUCTION

At present, close stellar binaries with short orbital periods have already been studied extensively, whereas wide binaries are valuable objects to investigate for the sake of studying the origin and evolution of wide pairs aimed not only at determining stellar masses, but also at gaining insight into the evolution of stellar matter and Galactic dynamics. Furthermore, orbit determination (refinement) of visual binaries in the solar neighborhood brings us closer to solving the current problems in astronomy—the study of these stars as possible parent objects for finding eventual exoplanets. Thus, in the by Schakht et al. [1], calculations of the habitable zone boundaries around selected stars from the Pulkovo research program were performed, and estimates of the astrometric signal depending on the gravitational influence of hypothetical planets were obtained.

The orbital motion studies in binary stars are traditionally aimed at the determination of their masses and dynamical parallaxes. However, this is true only for stars where a large arc of the orbit is observed. In the case of wide pairs with periods of several hundred or several thousand years, we have the data for only a short arc of the entire orbit. Thus, we have to address the inverse problem: with spectral types of its components, we estimate their masses in accordance with the mass–luminosity relation, and try to calculate the elements of Keplerian orbit. On the other hand, other authors quite often give different estimates of the spectral classification of the studied star components. In addition, different methods give various estimates of their masses with a difference of 0.5 solar masses or more.

It is known that long-period binary stars with a separation between the components of more than 100 AU are the least studied objects. In the 6th catalog of orbits of visual binaries [2], they make up only 7%. In the paper by Kiselev and Romanenko [3], it is suspected that their orbits are steeply inclined to the Galactic plane. Perhaps this is due to the still unexplored features of its structure. To study this issue, it is necessary to have sufficient statistical material.

The problem regarding the preferred direction of the orbital pole distribution of visual binaries in the solar neighborhood is currently an urgent problem. Thus, Agati et al. [4] analyzed the data of the Sixth Catalog of Orbits of Visual Binary Stars [2] and

showed that the poles of 20 systems located within 8 pc from the Sun concentrate toward $(L, B) \sim (46°, +37°)$, whereas the concentration of poles disappears for the full sample of 51 systems located within 18 pc. Agati et al. [4] concluded that the reality of the anisotropy cannot be assessed with certainty at this stage, because the number of systems with known orbital elements and with known position of the orbit's ascending node is too small. Therefore, it is important to increase the amount of these data and continue analyzing the results.

The study of the dynamics of wide stellar pairs with orbital periods of several thousand years is fundamentally different from the study of the dynamics of close binaries:

1. The first epochs of positional observations of wide pairs have significantly worse errors than modern observations. Moreover, the percentage of crude errors is very high, so the introduction of weights (for example, by the observation method—visual, photographic, speckle-interferometric, CCD or space-borne) does not correct the situation. On the other hand, the first epochs—the beginning of the observed arc—are decisive in determining such orbits.

2. At the present time, the most popular methods to determining the orbits (e.g., Hartkopf et al. [5], Hale [6], Mason et al. [7], Baidin et al. [8], Izmailov [9]) are based on the Thiele–Innes method, assuming that the observations fall on different phases along the entire orbit and cover the entire visible ellipse. Therefore, the period P, the eccentricity e and the time of periastron passage T_{peri} are known. However, according to the entire history of positional observations of binary stars (180–200 years), wide pairs passed a phase of 3–5% of their ellipse in their relative orbital motion, and the indicated values were not determined in advance. Thus, the use of this method is not justified. The same applies to the new algorithm by Blunt et al. [10], which is mainly associated with the fitting of the exoplanet orbits.

3. All of the above methods for obtaining the binary orbits lead to a two-valued solution based on the certainty of the ascending node. Only additional studies involving the radial velocities of the components (and this is not always a feasible task for both close and wide pairs) lead to unambiguity.

4. The methods developed for calculating the orbits of close pairs often lead to obtaining long-period orbits corresponding to the sum of component masses in several tens of solar masses, significantly exceeding the value determined by the mass–luminosity relation. The papers by Mason et al. ([7], ADS 7724, 17 $M_\odot$) and Izmailov ([9], see below) show such examples. However, the authors do not comment on these circumstances in any way. In the paper by Baidin et al. [8], photometric data are used, and this problem is solved by introducing the corresponding coefficient.

Figure 2a shows the observations of component B relative to the main star A of the ADS 246 pair according to the Washington Visual Double Star Catalogue (WDS [11]). For 150 years, observations have covered a 12° arc. This arc can be described by probable orbits with periods from 800 to 8000 years [9], if we use only positional observations, that is, the classical approach to determining the orbit. If we take the Gaia DR2 parallax [12], then the corresponding sums of masses will vary from 0.51 to 12.0 $M_\odot$. For ADS 2757 and ADS 12169 studied in this paper, this scatter according to Izmailov's orbits [9] ranges from 3.5 to 2600 and from 2.5 to 3700 $M_\odot$, respectively. A different approach is needed to reduce this uncertainty. It should be noted that, bearing in mind the errors of visual observations of the 19th to early 20th centuries, classical methods give reliable results for determining the orbits on arcs of at least 25° (see Baidin's study [13]) and do not work in this case.

Thus, at present, there is a need to develop a standard formal method for determining the orbits of wide pairs, considering all these points.

2. AMP-METHOD AND ITS MODIFICATION

The parameters of apparent motion are called the following values determined at the mean time moment T_0: ρ and θ are the polar coordinates of satellite B relative to the main star A, μ and ψ are the magnitude and positional angle of the apparent relative motion.

In the method of apparent motion parameters (AMP), developed by Kiselev and Kiyaeva [14–18], we don't only consider disparate positional observations of different authors, but also a dense homogeneous series. This is necessary to obtain not only the relative position of the components, but also the velocity in the sky plane. In addition, we use the relative line-of-sight velocity obtained from literature data (spectral observations). To correctly calculate the spatial velocity, the accuracy of determining the radial component should be of the order of 0.1 km/s. Having determined the spatial vectors of position $\vec{R}$ and velocity $\vec{V}$ at a certain mean time moment (Laplace's idea), we obtain a family of orbits that depend on the spatial separation between the components r:

$$r_{\min} = \frac{\rho}{\pi_t} \le r < r_{\max} = \frac{8\pi^2}{V^2} M_{AB}. \qquad (1)$$

Here, on the left is the minimum value of the distance r (the value of the vector's $\vec{R}$ projection onto the plane of the sky), on the right is the maximum value of r allowing elliptical motion according to the energy integral in the two-body problem, π_t is the trigonometric parallax, M_{AB} is the total mass of the components (in units of $M_\odot$), and V is the spatial velocity of satellite B relative to the main star A (in AU/year),

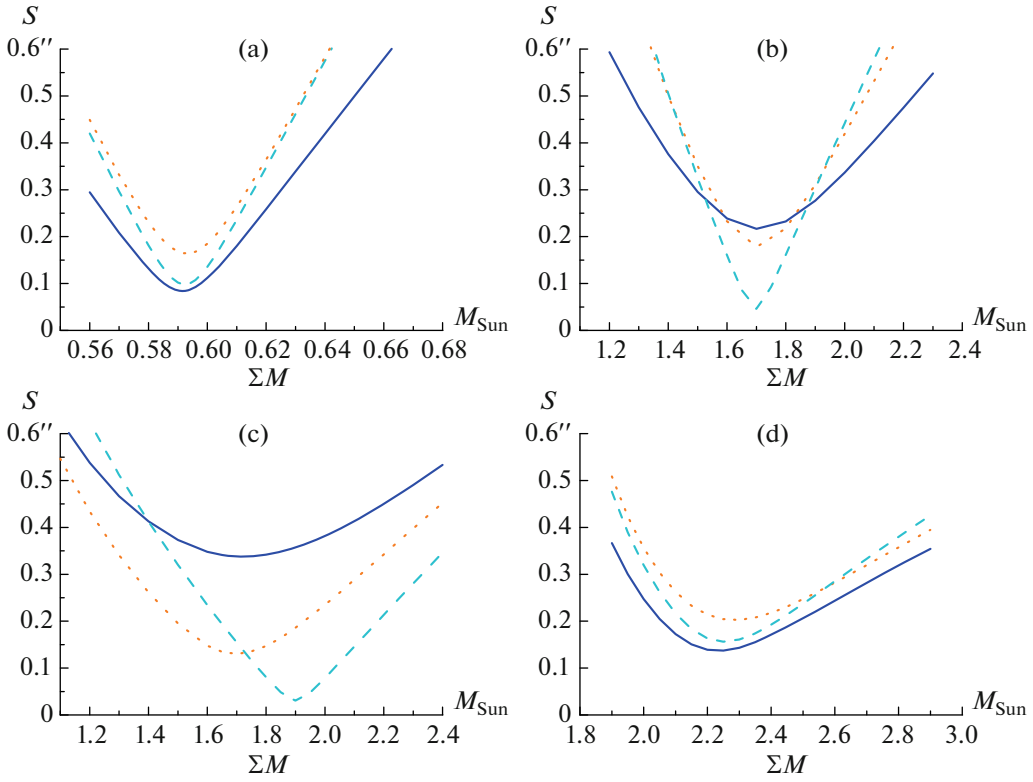

Fig. 1. Seeking a solution for ADS 246 (a), ADS 2757 (b), ADS 10386 (c), and ADS 12169 (d). Dependencies $S = f(M_{AB})$ for different bases are given. Solid (blue) and dashed (cyan) lines are the results obtained from the combined series (photo + CCD) and only from Pulkovo CCD observations, respectively. The dotted line (orange) is the result obtained from the Gaia DR2 data [12].

which is determined from positional and spectral observations:

$$V^2 = \left(\frac{\mu}{\pi_t}\right)^2 + \left(\frac{\Delta V_r}{4.74}\right)^2, \qquad (2)$$

where $\Delta V_r = V_{rB} - V_{rA}$ is the relative radial velocity of the components in km/s.

Let us denote by β the inclination angle of the vector $\vec{R}$ to the sky plane at the mean time moment T_0. Its value can be determined from the relationship:

$$r\cos\beta = \frac{\rho}{\pi_t}, \qquad (3)$$

where r must satisfy condition (1) for given ρ, π_t, V, and M_{AB}. The angle β is in the range from the minimum $\beta_{\min} = 0$ to the maximum $\pm\beta_{\max}$.

From relation (3), we obtain two values $\pm\beta$ corresponding to the location of B relative to A at the time moment T_0 behind the plane of the sky ($\beta > 0$) or in front of it ($\beta < 0$). As a result, we obtain two equally possible orbits that are dynamically identical and geometrically different.

If there are observations that are sufficiently distant from the main (basic) series, one can determine the only solution from the family of orbits by choosing the angle β that best suits all observations as follows (see [17, 18]).

First, we examine a worldwide series of disparate observations, considering the points described in the Introduction, and carefully analyze it. As for the first epochs, our practice of dynamic studies of more than 50 visual binaries (see the review by Romanenko and Kalinichenko [19]) showed that W. Struve's observations in 1830–1835 are the most reliable among observations of the early 19th century. At the same time, earlier observations of this scientist obtained with another instrument may contain crude errors, especially in the positional angle. To identify crude errors, we compare all global observations with the preliminary orbit separately for the angular distance ρ and separately for the positional angle θ. Such an orbit is necessary, since the observed arc of the ellipse of more than 3° is nonlinear, and the motion along it is uneven. Next, we use the well-known 3σ-criterion for rejecting such errors.

We divide the remaining positional observations into time intervals of 40 years. For mean time

moments, we obtain polar coordinates (ρ, θ) in these regions to obtain the clearest positions with different phases. This is how we compose the comparison control series.

Furthermore, to choose the best solution from the family of orbits, we use not a direct comparison of ephemeris with observations, but an agreement between the Thiele–Innes elements (A, B, F, G) that can be calculated from the geometric orbital elements (a, i, ω, Ω) without invoking any observations and from the dynamic elements (P, T, e) using the control comparison series. For more details, see the work of Kiyaeva [20]. A criterion is the minimum of the function S:

$$S = \sqrt{\Delta A^2 + \Delta B^2 + \Delta F^2 + \Delta G^2}. \quad (4)$$

Here, ΔA, ΔB, ΔF, and ΔG are the differences of the Thiele–Innes elements derived in two ways. The Thiele–Innes elements are the direction cosines of the measured and orbital coordinate axes, multiplied by the semi-major axis of the orbit a, so if the orbit is well agreed, then $S < Err_a$.

In contrast to the direct comparison of the observations and ephemerides, the function S is more sensitive. In this case, there is no need to assign the weights to specific heterogeneous observations that necessarily introduce some subjectivity, but it is important to have several reliable points widely spaced along the entire arc near the middle of the observation band. In other words, we compare two arcs: an ephemeris derived from a base arc with a given angle β and mass M_{AB}, and a flattened global observed arc. Such a comparison algorithm makes it possible to investigate both the entire family of orbits, depending on β for a fixed mass, and to set the sum of the component masses within the limits of interest to us with a certain step, to reveal the dependence of the function S on mass (its minimum) and to compare with the mass corresponding to the mass–luminosity relation.

In the AMP method, the errors of the obtained orbit elements (a, P, e, ω, i, Ω, and T_{peri}) are calculated by varying each of the initial parameters (ρ, θ, μ, ψ, π, ΔV_r, and β) within its error [14]. And, if earlier, the errors of the relative radial velocity and parallax had the greatest influence on the orbit elements, then the use of the Gaia DR2 [12] results led to a significant decrease in the influence of the error of the latter.

From high-resolution observations of Gaia DR2 [12] of positions and proper motions for each component, one can obtain the parameters of the apparent motion and a family of orbits, then the best orbit [17]. However, for each given sum of component masses, there will be its own family and its own best orbit. In this paper, we propose to analyze not only the family of orbits obtained from the Gaia DR2 basis, but also from the basis of dense homogeneous ground-based series—Pulkovo observations. The coincidence of the orbits determined from different bases leads, in our opinion, to the final orbit, and to an increase in its reliability. The system's mass corresponding to this orbit is also definitively determined. The coincidence limits of orbits give estimates of the error of this value.

3. OBSERVATIONS

The components of the stars studied here (ADS 246, 2757, 10386, and 12169) are red and yellow dwarfs from 6 to 11^m with distances between them from 7″ to 35″. These pairs are included in the Pulkovo research program [21], with its CCD observations continued with a 26-inch refractor [22, 23]. In this paper, we used CCD observations from 2003 to 2019, which can be downloaded from the Strasbourg Data Center or from the Pulkovo Observatory astrometric database system.[1] Here, we provide fragments of these tables: Table 1 gives individual observations (for calculations), and Table 2 presents average annual (to demonstrate the results and figures). With the emergence of new data [12] and new algorithms [17], it became possible to obtain the AMP orbits of these binaries from the Gaia data and compare them with the AMP orbits obtained from the Pulkovo series.

Table 3 shows the stellar magnitudes and spectral types of the components of the studied stars according to WDS [11], the characteristics of the available short arcs of observations of these stars: their duration and change in the position angle for global observations [11], photographic [21] and CCD observations (Table 1) on the 26″ refractor of the Central (Pulkovo) Astronomical Observation of Russian Academy of Sciences (CAO RAS), as well as unit weight errors for Pulkovo series. This Table also shows data on the series of the US Naval Observatory in Washington: photographic USNO and speckle interferometric WSI according to [11], if available. Note that the arc length of global observations ranges from 3° to 20°.

The review [19] provides a comparison similar series for 28 stars of the Pulkovo research program; it is shown that the accuracy of CCD observations is 5 times higher than the accuracy of photographic ones. Therefore, in the future, we began to use them as the main arc (basis) for some stars of the Pulkovo program (see, for example, the studies of ADS 12889 = 17 Cygnus FG [24], arc of ~5°). In the AMP method, not only the accuracy of the observed main arc (basis) is important, but also its length. The arc of ground-based observations of the achieved accuracy less than 3° in length does not lead to reliable results. Therefore, for slowly moving stellar pairs, we supplemented the existing base arc with reliable observations from the WDS catalog [11] (see, for example, [16, 17, 24]).

Table 4 shows data from the Gaia DR2 catalog [12]: parallaxes, proper motions, and radial velocities for

[1] http://izmccd.puldb.ru/vds.htm

Table 1. Results of individual CCD observations for 4 visual binaries performed at the Pulkovo 26-inch refractor (fragment)

ADS	Date, epoch	$N1$	ρ, arcsec σ_ρ, arcsec	θ, deg σ_θ, deg	$\sigma_{\rho 1}$, arcsec	$\sigma_{\tau 1}$, arcsec	Δt
246	2003 12 08	17	35.0288	64.3694	0.0202	0.0336	5.48
	2003.935		±0.0051	±0.0137			
	2003 12 30	17	35.0328	64.3837	0.0104	0.0283	5.48
	2003.995		±0.0026	±0.0116			
	2004 01 02	17	35.0298	64.3977	0.0319	0.0316	5.48
	2004.003		±0.0080	±0.0129			
	2004 11 14	17	34.9811	64.5696	0.0247	0.0287	5.48
	2004.872		±0.0062	±0.0117			
	2004 12 12	17	34.9771	64.5558	0.0288	0.0268	5.48
	2004.948		±0.0072	±0.0110			

The columns of the table contain: ADS is the number of the star under study from Aitkin's catalog; Date (in the year–month–day format) and corresponding epoch (J2000) in years; $N1$ is the number of CCD images; ρ is the distance between components in arc seconds; θ is the positional angle in degrees; σ_ρ is the distance error, σ_θ is the position angle error; $\sigma_{\rho 1}$ and $\sigma_{\tau 1}$ are measurement errors for one image in the radial and tangential directions, where $\sigma_{\tau 1} = (\pi/180^\circ)\rho\sigma_{\theta 1}$; and Δt is the exposure time in seconds.

Table 2. Results of annual average CCD observations of 4 visual binaries with the 26-inch refractor of the Pulkovo Observatory (fragment)

ADS	Epoch	$N2$	ρ, arcsec σ_ρ, arcsec	θ, deg σ_θ, deg	$\sigma_{\rho 1}$, arcsec	$\sigma_{\tau 1}$, arcsec
246	2003.978	3	35.0318	64.3841	0.0017	0.0067
			±0.0012	±0.0077		
	2004.910	2	34.9794	64.5622		
	2005.660	5	34.9094	64.5922	0.0075	0.0108
			±0.0038	±0.0088		
	2006.788	7	34.8725	64.7094	0.0162	0.0102
			±0.0066	±0.0068		
	2007.731	6	34.7896	64.7355	0.0139	0.0100
			±0.0062	±0.0074		

The designations are as in Table 1, $N2$ is the number of normal places.

each component. The proper motions of the components are quite significant and have the same direction, the physical connection in pairs is beyond doubt. The radial velocities of Gaia in comparison with the data from [25–27] are as follows: for the first pair, there are no measurements of component B (possibly too weak, see Table 3). For the second pair, the error in the radial velocity of component B is too large (it is known that this component is spectral binary. The table gives the value of the radial velocity of the mass center according to the spectral orbit [26]). This means that the radial velocity obtained by Gaia is instantaneous and cannot be used. The errors for the components of the third and fourth pairs are worse than those of the literature data (see Table 4). As a result, it was not possible to use the Gaia radial velocity data.

The most recent study of solar-type stars in 2018 [28] contains the results of determining the radial velocities of the components of ADS 2757 and 10386. However, the corresponding spectral observations were carried out in 1980–1990, that is, in the same time period as in [26, 27], but with less accuracy. Therefore, we will focus on the data of these works (see Table 4).

Table 5 provides the parameters of the apparent motion for the studied stars using different bases, the parallaxes and relative radial velocities, and the arc length of the corresponding base. Note that for ADS 246, we supplemented our Pulkovo series with photographic USNO observations [11]. For the AMP method, it is important that the USNO series, like the Pulkovo one, is homogeneous. The point is that this fast wide pair was included in the Pulkovo program of photographic observations with a 26-inch refractor

Table 3. Characteristics of the positional series for 4 studied stars

ADS/WDS	m_v	Sp	ρ, arcsec	Series	T_1, yr	T_2, yr	n	Δθ, deg	$\sigma_{\rho 1}$, arcsec	$\sigma_{\tau 1}$, arcsec
246	8.13	M2V		WDS	1860	2015	123	**12.3**		
00184+4401	11.04	M3Ve	35.0	*USNO*	*1964*	*1976*	*46*	*1.1*	*0.0110*	*0.0232*
				Photo	1994	2006	7	0.1	0.0633	0.3192
				CCD	2003	2019	145	1.4	0.0100	0.0085
2757	8.12	K2V		WDS	1822	2011	125	**10.0**		
03470+4126	8.82	K3V	7.4	Photo	1960	2001	101	2.5	0.0479	0.0379
				CCD	2004	2019	52	1.1	0.0087	0.0071
10386	8.85	K6V		WDS	1830	2012	42	**3.1**		
17102+5430	9.21	K6V	22.0	Photo	1961	2002	27	0.9	0.0202	0.0241
				CCD	2004	2018	31	0.4	0.0128	0.0094
12169	6.57	G2V		WDS	1819	2015	297	**20.6**		
19121+4951	6.75	G3V	7.8	Photo	1961	1999	97	4.9	0.0234	0.0133
				CCD	2003	2019	157	2.4	0.0104	0.0042
				WSI	*2000*	*2014*	*25*	*3.5*	*0.0551*	*0.0327*

The columns of the table show: ADS and WDS are the numbers of the studied stars from Aitkin's and WDS catalogs [11]; m_v and Sp are the stellar magnitudes and spectral types of the components according to [11]; ρ is the average angular distance between components; T_1 and T_2 are the initial and final observation epochs; n is the number of observations; Δθ is the change in the positional angle of satellite B relative to the main star A during the interval of these observations; $\sigma_{\rho 1}$ and $\sigma_{\tau 1}$ are the errors in the unit of weight in the radial and tangential directions, similar to Table 1. The column "Series" shows the series: WDS—global observations [11], Photo—photographic observations with the 26″ refractor of the GAO RAS [21], CCD—the CCD observations (Table 1) with the 26″ refractor of the CAO RAS. Photographic (*USNO*) and speckle interferometric (*WSI*) observation series of the US Naval Observatory according to [11] are italicized.

Table 4. GAIA DR2 data on the studied visual binaries

ADS	π, mas	μ_x, mas/yr	μ_y, mas/yr	V_r, km/s	V_r*, km/s	n*	Reference
246A	280.69 ± 0.04	2891.5	+411.9	+11.51 ± 0.14	+11.97 ± 0.22	11	[25]
246B	280.79 ± 0.05	2863.2	+336.5	–	+10.98 ± 0.16	7	[25]
B–A	280.73 ± 0.07			–	–0.99 ± 0.27		
2757A	41.83 ± 0.04	+598.0	–1243.9	+50.87 ± 0.14	50.18 ± 0.11	20	[26]
2757B	41.36 ± 0.05	+588.7	–1262.0	+50.00 ± 1.91	(50.80 ± 0.06)	43	[26]
B–A	41.64 ± 0.06			–0.87 ± 1.92	+0.62 ± 0.13		
10386A	47.05 ± 0.03	+81.9	–110.6	+2.95 ± 0.17	+2.69 ± 0.13	11	[27]
10386B	47.07 ± 0.02	+86.3	–103.2	+2.19 ± 0.38	+1.73 ± 0.12	11	[27]
B–A	47.06 ± 0.04			–0.76 ± 0.42	–0.96 ± 0.18		
12169A	39.56 ± 0.02	–210.6	+621.2	–40.99 ± 0.17	–41.26 ± 0.13	9	[27]
12169B	39.60 ± 0.02	–185.9	+630.2	–41.86 ± 0.26	–41.73 ± 0.13	9	[27]
B–A	39.58 ± 0.03			–0.87 ± 0.31	–0.47 ± 0.18		

The columns of the table show: π, μ_x, μ_y, and V_r are the parallax, proper motions, and radial velocity with errors for each component according to [12], respectively. V_r* and n* are the radial velocity and the number of spectral observations according to the given references. For ADS 2757, the radial velocity of the mass center of component B is given in parentheses according to the spectral orbit [26]. In the third line, for each binary, the weighted average parallax and the relative radial velocity of the components are given $\Delta V_r = V_{rB} - V_{rA}$.

just when we learned the results of determining the radial velocities of its components [25]. However, the epoch of photography is over, and we have not had time to accumulate a sufficient number of Pulkovo observations. Fortunately, the epoch of Pulkovo CCD observations continues.

4. RESULTS

For each studied binary all the necessary data such as the parameters of apparent motion, parallax and relative radial velocity (see Table 5) and setting $\beta = 0 \pm 90°$, we obtain an orbit family for each fixed mass and each basis. Comparing the Thiele–Innes

Table 5. Initial data for determining the AMP orbits of the studied stars

ADS	T_0, year	ρ, arcsec	$\theta_{2000.0}$, deg	μ, mas/yr	$\psi_{2000.0}$, deg	π_G, mas	ΔV_r, km/s	Δθ, deg	Base
246	1991.8	35.641	63.307	74.5	194.9	280.73	–0.99	4.9	UCCD
		± 0.002	± 0.003	± 0.1	± 0.1	± 0.07	± 0.27		
	2011.4	34.607	65.104	80.1	199.9	280.73	–0.95	1.5	CCD
		± 0.001	± 0.001	± 0.2	± 0.1	± 0.07	± 0.27		
	2015.5	34.37823	65.4466	80.49	200.5	280.73	–0.95	0.0	G18M
		± 0.00004	± 0.0001	± 0.06	± 0.1	± 0.07	± 0.27		
2757	1989.9	7.315	54.145	17.7	206.3	41.64	0.62	3.8	PCCD
		± 0.003	± 0.014	± 0.2	± 0.4	± 0.06	± 0.13		
	2011.4	6.953	55.654	20.1	208.5	41.64	0.59	1.1	CCD
		± 0.001	± 0.007	± 0.2	± 0.6	± 0.06	± 0.13		
	2015.5	6.89037	55.9510	20.42	207.1	41.64	0.56	0.0	G18T
		± 0.00004	± 0.0003	± 0.11	± 0.3	± 0.06	± 0.13		
10386	1990.1	22.191	133.678	8.8	32.1	47.06	–0.96	1.3	PCCD
		± 0.005	± 0.012	± 0.2	± 1.5	± 0.04	± 0.18		
	2011.4	22.154	133.200	8.7	29.0	47.06	–0.96	0.4	CCD
		± 0.002	± 0.003	± 0.4	± 2.4	± 0.04	± 0.18		
	2015.5	22.14408	133.1073	8.55	30.9	47.06	–0.96	0.0	G18T
		± 0.00003	± 0.0001	± 0.08	± 0.6	± 0.04	± 0.18		
12169	1990.7	7.654	207.866	25.7	71.6	39.58	–0.47	7.5	PCCD
		± 0.001	± 0.010	± 0.1	± 0.2	± 0.03	± 0.18		
	2011.6	7.264	204.901	27.1	70.3	39.58	–0.37	2.4	CCD
		± 0.001	± 0.003	± 0.1	± 0.2	± 0.03	± 0.18		
	2015.5	7.19678	204.3334	26.24	70.0	39.58	–0.36	0.0	G18T
		± 0.00004	± 0.0002	± 0.06	± 0.2	± 0.03	± 0.18		

The columns of the table show: T_0 is the average time of observations; parameters of apparent motion: ρ is the angular separation between components, θ is the positional angle of relative position, μ is the apparent speed of relative motion, ψ is the positional angle of relative motion; additional parameters: π_G is the parallax and ΔV_r is the relative radial velocity (see Table 4); Δθ is the change the positional angle; bases: UCCD—a combined series of photographic observations of the USNO observatory [11] and CCD observations in Pulkovo (see Table 1), CCD—a series of CCD observations at Pulkovo (see Table 1), G18—data from Gaia DR2 (2018) [12]. In the designation of the Gaia basis, the last letter corresponds to the first letter in the name of the first author of the publication of the radial velocities of this star (M—Marcy [25] and T—Tokovinin [26, 27]). The relative radial velocity is corrected for the orbital motion for the time interval from the 1990s, when the indicated radial velocity observations were made, until the time T_0; for ADS 10386 this correction was not required.

elements of each orbit using the control series of observations and without it by Eq. (4), we obtain the dependence of the function $S = f(M_{AB})$. The revealed dependences for four studied stars and different bases are shown in Fig. 1. For three of them, the correspondence of minima on different bases is quite definite and amounts to: 0.59 $M_\odot$ for ADS 246, 1.70 $M_\odot$ for ADS 2757, and 2.25 $M_\odot$ for ADS 12169. For the slowest pair of ADS 10386, the minimum for the CCD basis differs slightly from the coinciding minimums obtained for the most reliable duration (PCCD) and accuracy (G18T) bases. Finally, we choose the sum of the masses 1.70 $M_\odot$ obtained from the latter two bases.

With the sum of masses obtained in this way, we reveal the dependence of the function $S = f(\beta)$ and its minimum. The Keplerian orbital elements corresponding to this β and this basis are compared with the orbital elements obtained in a similar way from another basis. The coincidence of the orbital elements in three different bases leads to the final result. However, each time, one should calculate the ephemeris relative radial velocity at the time moment T_0 so that its value at the average time moment of the spectral observations corresponds to the publication. Therefore, Table 5 gives ΔV_r already considering orbital motion.

Table 6 shows the AMP orbits obtained in this paper from different bases, in the lower rows for each

Table 6. Elements of improved AMP orbits of 4 studied stars

β, deg	*A*, AU	*P*, yr	*e*	ω, deg	*i*, deg	Ω, deg	T_{peri}, yr	*S*, arcsec	σ_ρ, mas σ_τ, mas	Base
ADS 246 ($\pi_G = 280.73$, $M_{AB} = 0.59$)										
−15	97	1242	0.48	353	53	232	2404	0.08	124.6	UCCD
±2	±11	±201	±0.14	±11	±6	±3	±52		125.1	
−15	96	1219	0.51	350	52	233	2380	0.32	135.5	CCD
±3	±10	±189	±0.13	±12	±6	±3	±45		126.5	
−16	96	1220	0.50	351	53	233	2387	0.20	127.3	G18M
±2	±10	±187	±0.13	±12	±6	±3	±42		126.4	
–	96	1226	0.50	352	53	232	2389	–	–	Weighted
	±12	±236	±0.16	±15	±7	±4	±57		–	average
ADS 246 ($\pi_{Hip} = 279.0$, $M_{AB} = 0.56$)										
0	96	1253	0.59	331	46	243	2327	–	–	UPhoto [29]
	±11	259	±0.19	±32	±11	±25	±81		–	
ADS 2757 ($\pi_G = 41.64$, $M_{AB} = 1.70$)										
+16	125	1073	0.80	181	51	41	2253	0.24	55.4	PCCD
±3	±3	±44	±0.04	±4	±5	±2	±18		76.4	
+13	125	1077	0.82	176	46	43	2235	0.09	55.2	CCD
±2	±2	±30	±0.03	±4	±5	±2	±11		70.4	
+13	125	1075	0.81	176	43	42	2238	0.09	55.3	G18T
±3	±3	±34	±0.03	±4	±5	±2	±11		74.8	
–	125	1075	0.81	178	47	42	2239	–	–	Weighted
	±3	±45	±0.04	±5	±6	±3	±17		–	average
ADS 2757 ($\pi_{Hip} = 41.0$, $M_{AB} = 1.7$)										
+3	126	1090	0.87	168	31	49	2215	–	–	Photo [30]
	±3	±40	±0.05	±13	±15	±10	±24		–	
−3	126	1090	0.89	157	23	60	2209	–	–	Photo [30]
	±3	±40	±0.02	±57	±13	±57	±5		–	
ADS 10386 ($\pi_G = 47.6$, $M_{AB} = 1.70$)										
−5	324	4472	0.47	2	132	318	4083	0.34	95.0	PCCD
±8	±26	±544	±0.11	±16	±6	±6	±283		95.8	
−8	325	4483	0.47	7	131	320	4131	0.18	98.9	CCD
±4	±26	±542	±0.11	±14	±5	±5	±326		100.4	
−10	324	4481	0.47	13	130	322	4237	0.30	92.7	G18T
±4	±26	±532	±0.11	±8	±5	±3	±188		104.0	
–	324	4478	0.47	10	131	321	4179	–	–	Weighted
	±32	±660	±0.13	±16	±7	±6	±333		–	average
ADS 10386 ($\pi_{Hip} = 47.0$, $M_{AB} = 1.3$)										
0	345	5610	0.39	347	129	314	4360	–	–	Photo [29]
	±43	±1065	±0.17	±30	±6	±11	±488		–	
ADS 12169 ($\pi_G = 39.58$, $M_{AB} = 2.25$)										
–43	378	4893	0.49	317	123	66	2407	0.14	129.6	PCCD
±1	±20	±380	±0.02	±9	±1	±2	±17		±92.9	
–43	378	4890	0.53	317	125	66	2379	0.27	119.1	CCD

Table 6. (Contd.)

β, deg	*A*, AU	*P*, yr	*e*	ω, deg	*i*, deg	Ω, deg	T_{peri}, yr	*S*, arcsec	σ_ρ, mas σ_τ, mas	Base
±1	±18	±361	±0.02	±8	±1	±2	±13		±97.0	
–46	377	4876	0.49	317	123	66	2412	0.20	130.1	G18T
±1	±23	±442	±0.02	±9	±1	±2	±17		±94.3	
–	377	4887	0.50	317	124	66	2395	–	–	Weighted
	±25	±485	±0.02	±11	±2	±3	±19		–	average
ADS 12169 ($\pi_{vAlt} = 42.0$, $M_{AB} = 1.8$)										
–38	316	4186	0.55	332	129	69	2395	–	–	Photo [15]
+38	316	4186	0.65	171	133	258	2369	–	–	Photo [15]

The columns of the table show: β is the angle between the position vector $\vec{R}$ at the moment T_0 and its projection onto the plane of the sky; *A*, *P*, *e*, ω, *i*, Ω, and T_{peri} are Keplerian elements of the orbits; *S* is the value of the function that characterizes the consistency of the orbit with the observations of the control series (according to formula (4); σ_ρ and σ_τ are the root-mean-square residuals obtained from all observations from the WDS (satisfying the 3σ-criterion) with equal weights that characterize the quality of this comparison series, M_{AB} is the sum of the component masses in units of the solar mass. Designation of bases: UPhoto—combined series of photographic observations of USNO [11] and Pulkovo [21] observatories, the rest designations see in Table 5. The final weighted average decision was made from those obtained in this paper.

Table 7. Orbital elements of 4 visual binaries under study

ADS	*P*, yr	*a*, arcsec	*i*, deg	Ω, deg	T_{peri}, yr	*e*	ω, deg	M_{AB}, $M_\odot$	Reference
246	1226.2	26.98	52.5	232.4	2389.0	0.50	351.5	0.59 ± 0.05	Present work
	±235.7	±3.40	±7.4	±3.8	±56.7	±0.16	±14.6		
	1619.9	34.48	54.4	79.9	2267.3	0.68	112.3	0.71	[9]
	±487.9	±8.51	±8.5	±22.3	±61.1	±0.21	±26.6		Unweighted
	1590.7	35.83	55.5	84.0	2250.7	0.72	108.7	0.82	[9]
	±514.7	±10.50	±9.6	±19.2	±51.3	±0.17	±17.4		Weighted
	2600.0	41.15	61.4	45.3	1745.0	0.0	0.0	0.47	[31]
2757	1075.3	5.21	46.8	41.7	2239.2	0.81	177.7	1.70 ± 0.3	Present work
	±45.0	±0.14	±5.8	±3.0	±16.9	±0.04	±4.6		
	1551.2	16.00	84.4	39.3	1687.1	0.77	277.7	23.7	[9]
	±474.9	±5.95	±2.3	±1.6	±44.1	±0.15	±11.3		Unweighted
	2275.5	22.79	85.4	37.7	1636.2	0.83	282.8	31.7	[9]
	±904.6	±10.31	±2.7	±2.1	±65.4	±0.13	±13.4		Weighted
10386	4478.4	15.26	130.7	320.7	4178.6	0.47	9.8	1.70 ± 0.4	Present work
	±660.4	±1.49	±6.5	±6.1	±333.0	±.13	±16.1		
12169	4887.4	14.94	123.7	65.8	2394.8	0.50	317.0	2.25 ± 0.5	Present work
	±484.8	±0.98	±1.6	±2.5	±19.4	±0.02	±11.0		
	1514.0	15.29	100.8	241.7	1447.8	0.65	269.3	25.1	[9]
	±634.1	±7.64	±5.9	±4.5	±180.5	±0.27	±28.6		Unweighted
	1459.1	12.95	104.8	251.0	2604.9	0.67	247.2	16.5	[9]
	±1194.1	±8.28	±9.3	±12.8	±963.7	±0.26	±32.6		Weighted
	3100.0	12.75	119.1	255.2	2520.0	0.50	186.1	3.48	[6]

M_{AB} is the sum of the component masses, for AMP orbits, it was determined from the analysis of the coincidence of the family orbits obtained from different bases (this work). For other orbits, it was recalculated according to Kepler's third law taking into account the Gaia DR2 parallax (see Table 5).

Table 8. Orbital parameters in the galactic frame

ADS	β, deg	LQ	BQ	LP	BP	Base
246	−15	345	57	9	−31	UCCD
	±2	±8	±5	±12	±1	
	−15	343	58	6	−30	CCD
	±3	±9	±5	±13	±2	
	−16	344	58	7	−30	G18M
	±2	±8	±5	±12	±2	
	–	344	58	7	−31	Weighted average
		±10	±6	±15	±2	
	0	325	60	350	−28	UPhoto [29]
		±13	±6	±14	±2	
2757	+16	284	5	348	−79	PCCD
	±3	±5	±2	±4	±3	
	+13	289	5	343	−82	CCD
	±2	±5	±2	±4	±3	
	+13	291	5	336	−82	G18T
	±3	±5	±2	±3	±3	
	–	288	5	341	−81	Weighted average
		±6	±2	±5	±4	
	+3	304	4	334	−86	Photo [30]
	−3	313	−1	325	−89	Photo [30]
10386	−5	110	−4	197	32	PCCD
	±8	±5	±5	±8	±11	
	−8	109	−6	195	35	CCD
	±4	±4	±5	±8	±10	
	−10	109	−7	193	40	G18T
	±4	±4	±4	±4	±6	
	–	109	−6	194	37	Weighted average
		±5	±6	±8	±11	
	0	115	−5	203	20	Photo [29]
12169	−43	41	−24	221	−66	PCCD
	±1	±1	±2	±20	±2	
	−43	43	−23	220	−67	CCD
	±1	±1	±2	±18	±2	
	−46	41	−25	220	−65	G18T
	±1	±1	±2	±19	±2	
	–	42	−24	220	−66	Weighted average
		±1	±2	±23	±2	
	−38	43	−19	185	−66	Photo [15]
	+38	129	+36	132	−54	Photo [15]

The orientation parameters of the orbits in the Galaxy coordinate frame are given: the longitude and latitude of the vectors of the orbital pole $\vec{Q}$ and of the periastron $\vec{P}$.

star—the previous orbits. Recall that to calculate the latter, other parallax values and the sum of the component masses were used. We consider the weighted average solution among those obtained in this paper to be the most reliable result. In some cases, Pulkovo CCD arcs (1°–2°) are currently insufficient. It is necessary to continue the dense homogeneous CCD-rows on the 26-inch refractor of Pulkovo.

Table 7 shows the final AMP orbits, the average orbits obtained by Izmailov [9] without weights and with weights, as well as the orbits of other authors: Lippincott [31] and Hale [6]. The sum of the component masses is also given, which for AMP orbits is determined from the analysis of the coincidence of the family orbits obtained from different bases (this paper). For other orbits, it is recalculated with the Gaia DR2 parallax [12]. The table shows that, according to [9], for the studied visual binaries, the introduction of weights of positional observations does not improve the errors in determining the orbits, the sums of the component masses significantly exceed the masses corresponding to the mass–luminosity relation.

The modified AMP method gives a more reliable result, since it uses a whole set of reliable data, both astrometric and astrophysical in nature: a dense series of positional observations, reliable parallaxes and radial velocities of components, reliable (smoothed) observations to select the best solution from the family of AMP orbits. The sums of the component masses obtained by this method, within the error limits, correspond to the mass–luminosity relation.

Table 8 shows the orientation parameters of the AMP orbits in the Galaxy coordinate frame: longitude and latitude of the orbital pole vectors $\vec{Q}$ and periastron $\vec{P}$. In three out of four cases, the orbits are steeply inclined to the Galactic plane ($|b_Q| \le 30°$). Thus, the inclination of the orbital planes to the Galactic plane exceeds 60°. In the case of ADS 246, we have $b_Q = +58° \pm 6°$, but the separation of the components of this pair is less than 100 AU.

5. COMMENTS

The binary star ADS 246 is the closest pair with very large proper motions of the components (see Table 4) and with the most confident orbital motion. Figure 2 shows the hypothetical (circular) Lippincott orbit of 1972 [31], our 2014 AMP orbit [29], as well as three practically coinciding AMP orbits obtained in this work from different bases (Tables 5 and 6). We can see that Lippincott's orbit deviates from modern observations, including those of Gaia observations. The orbit obtained this year differs little from the previous one [29], but it is more reliable. The total sum of the component masses $0.59 \pm 0.05\ M_\odot$ coincides

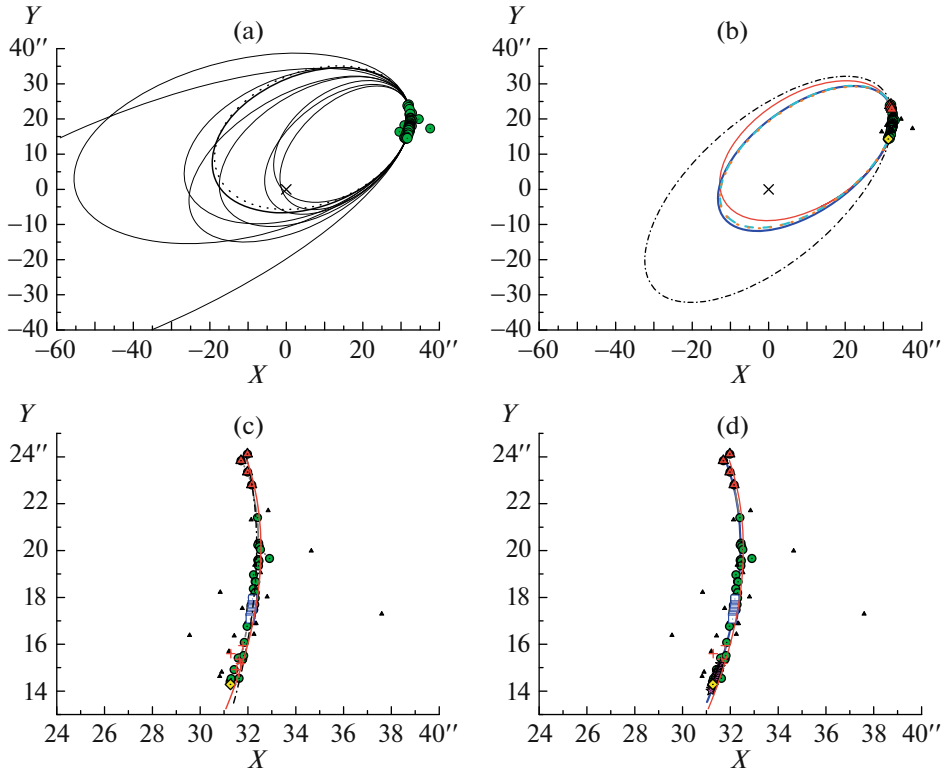

Fig. 2. Comparison of the orbits with observations for ADS 246. The *X*- and *Y*-axes point toward East and North, respectively, and the coordinate origin coincides with the component A (oblique cross). The circles are the relative observations of the B component adopted from WDS catalog [11], the triangles show the observations performed by O. Struve [11], small triangles correspond to observations adopted from WDS catalog [11] that did not pass the 3σ criterion by ρ or θ, squares mark photographic series of USNO observations [11], crosses present photographic observations at Pulkovo [21], the asterisks indicate the Pulkovo CCD observations (Table 2), and diamond marks space observations of Gaia DR2 2015 [12]. (a) Probable orbits of 2019. 8 orbits among 200 obtained by Izmailov [9] are shown, including orbits with the minimum (834 years) and maximum (7898 years) periods. The bold solid line shows the mean orbit without weights, the dotted line indicates the mean orbit with weights (see Table 7). (b) AMP orbits and 1972 orbit. Designations: dash-dotted line shows 1972 Lippincott orbit [31], solid (red) line marks 2014 AMP orbit [29], blue solid line, cyan dashed line and orange dotted line indicate AMP orbits obtained from different bases (see Tables 5 and 6), practically coinciding with each other, correspond to the sum of masses $M_{AB} = 0.59M_{\odot}$. (c) Preliminary 1972 and 2014 orbits. See designations above. Obviously, Lippincott's orbit deviates from modern observations. (d) Final AMP orbit. Designations: thick (blue) line shows ephemeris for 1860–2025 of the final orbit (see Table 6), practically coinciding with the AMP 2014 orbit (for other designations see above).

within the error with the value corresponding to the mass–luminosity relation.

The faint component of the visual binary ADS 2757 is a spectroscopic binary. Tokovinin et al. [26] determined its spectral orbit with a period of about 48 days and the sum of the component masses (considering the spectral satellite) 1.68 $M_{\odot}$. The best match of the AMP orbits obtained in this paper corresponds to the close value 1.70 $M_{\odot}$ (Fig. 3). The orbit obtained from Gaia DR2 data is less consistent with observations at the turn of the 19th to 20th centuries and reliable observations by W. Struve in 1830 (see Fig. 3d), which can be explained by the influence of the spectral satellite of component B. However, within errors, it agrees with the other two, determined by Pulkovo bases. The final one is considered the weighted average solution of the three (Table 6). Judging by the orbit elements, this orbit is closer to the preliminary orbit in 2000, corresponding to $\beta > 0$ [30]. Thus, it was possible to refine this orbit and obtain a unique solution for the plane of the sky. Figures 3a and 3c show both average Izmailov's orbits [9], corresponding to more than 20 $M_{\odot}$ (Table 7). Note that they both deviate from Struve's reliable observation in 1830.

ADS 10386 is an ordinary binary, in which the proper motions and radial velocities of the components are small, but, like the parallaxes, indicate the physical connection of the components (Table 4). The arc of global observations is only ~3°. According to the Pulkovo series of photographic observations in 1961–2002 (the arc in ~1°), a family of AMP-orbits was obtained in 2014 [29], the ephemeris of which practically coincide, it was not possible to choose a single

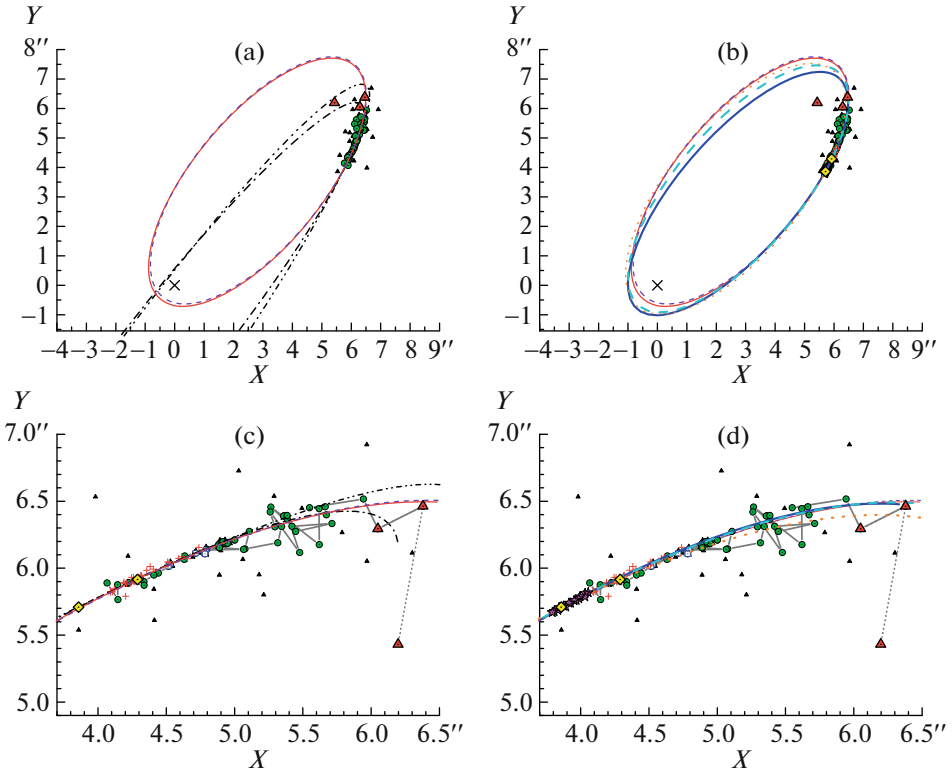

Fig. 3. Comparison of orbits with observations for ADS 2757. Designations: the triangles show observations of W. Struve in 1822–1851, the diamonds indicate Hipparcos space-born (1991) [11] and Gaia DR2 observations (2015) [12], other designations of observations are the same as in Fig. 2. (a) Preliminary orbits of 2000 and mean 2019 orbits. The thin solid and thin dashed lines mark AMP 2000 orbits, corresponding to $\beta > 0$ and $\beta < 0$ [30] (see Table 6), the dash-dotted line and the dashed line with two points are the mean orbits (with and without weights) obtained by Izmailov in 2019 [9], the corresponding sums of the component masses are equal to 24 and 32 $M_\odot$ (Table 7). (b) New AMP orbits. The thick solid (blue) line and thick dashed (cyan) line are the AMP orbits obtained from the combined Pulkovo series (photo + CCD) and only from the CCD observations, respectively, the dotted line is the AMP orbit obtained from the Gaia DR2 data [12] (orange). (c) Preliminary 2000 and 2019 orbits. Ephemeris for 1830–2025. AMP 2000 orbits, corresponding to $\beta > 0$ and $\beta < 0$, coincide with each other. It is obvious that the first observation by W. Struve in 1822 is not reliable and should not be considered when calculating the orbit. The mean 2019 orbits deviate from reliable Struve's observation on 1830. (d) New AMP orbits. Ephemeris for 1830–2025 are shown. AMP orbits obtained in this paper, corresponding to the sum of masses $M_{AB} = 1.7\ M_\odot$, see designations above.

solution. However, from Fig. 4a, we can see that the solution corresponding to $\beta = 0$ better describes the motion direction of component B. In addition, the deviation of the Pulkovo CCD observations (2004–2019) from these ephemeris is noticeable in this figure and improvement is required. According to the new algorithm, we corrected W. Struve's observation in 1830 at –0.5° in the positional angle θ and obtained practically coinciding AMP orbits in different bases, better describing all observations (see Fig. 4b).

The best of the new families of orbits, obtained from different bases according to the algorithm described by Kiyaeva [17], are in good agreement with observations. However, these are different orbits with different periods and eccentricities corresponding to different masses (Fig. 4c). We proceed from the assumption that the real orbit should be single with one period, one eccentricity and one mass. Figure 4d demonstrates AMP orbits obtained from different bases, coinciding with the sum of the component masses equal to 1.7 $M_\odot$, which is slightly higher than follows from the mass–luminosity relation (Table 6).

The components of ADS 12169 are yellow dwarfs. If their spectral classes were indicated as G5 and G5 earlier in the catalogs, then in the latest version of the WDS catalog—as G3V and G3V. Then, the value of the sum of the component masses should not be 1.8 $M_\odot$, which we used in 1996 [15], but 2.0 $M_\odot$. The best match of the new AMP orbits was obtained with 2.25 $M_\odot$ (Table 6), which, within the error limits, agrees with the mass–luminosity relation, but does not agree in mass with the Hale's results in 1994 [6] and Izmailov [9] (see Table 7). One can also note the correspondence of the geometric elements of the new weighted average orbit to the elements of the orbit in

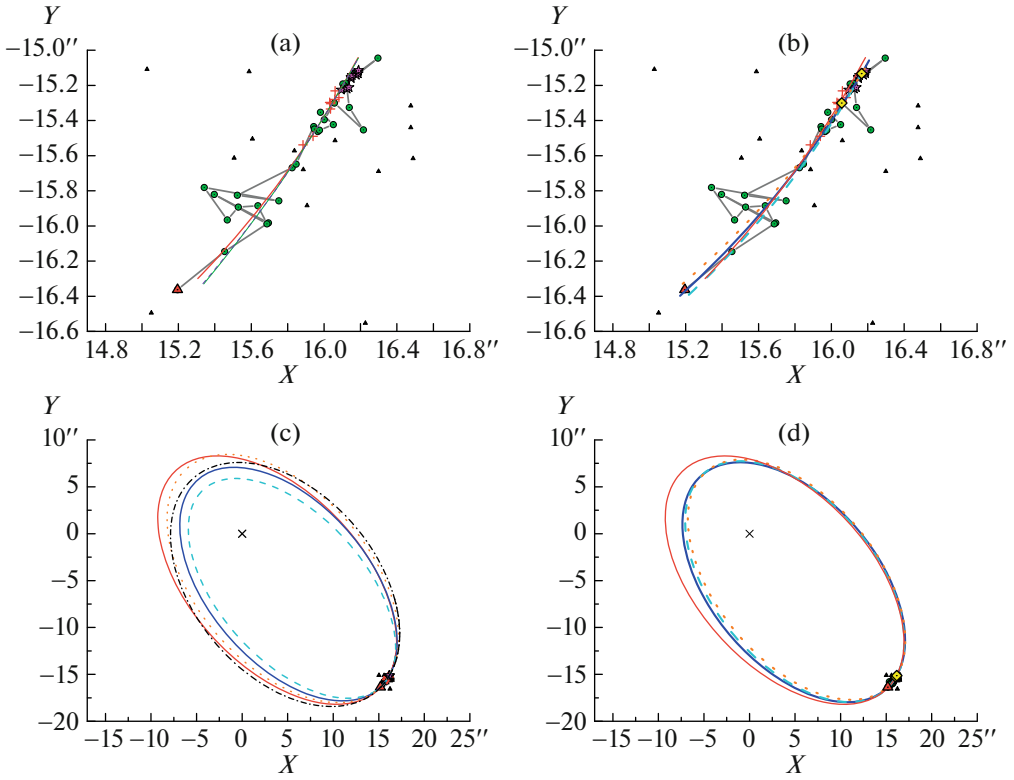

Fig. 4. Comparison of orbits with observations for ADS 10386. (a) Preliminary orbits of 2014. Designations: the triangle shows observation by W. Struve in 1830 adopted from WDS catalog [11], corrected to −0.5° in positional angle θ, the thin solid (red) line and thin dashed (violet) line indicate ephemeris for 1830–2025. The AMP orbits of the 2014 family [29], corresponding to $\beta = 0$, $\beta > 0$, and $\beta < 0$. The latter two coincide with each other, but poorly describe the direction of motion of component B. The deviation of Pulkovo CCD observations (Table 2) from these ephemeris is noticeable, improvement is required. (b) New AMP orbits corresponding to the sum of the component masses $M_{AB} = 1.7\ M_\odot$. For line designations, see Figs. 1 and 3. (c) The best AMP orbits obtained from different bases according to the algorithm [17]. Designations: the thin solid (red) line shows AMP orbit from the 2014 family [29], corresponding to the sum of component masses 1.3 $M_\odot$ (basis is Photo), the thick solid (blue) line marks the orbit obtained from the combined series (basis is PCCD, $M_{AB} = 1.7\ M_\odot$), the dashed (cyan) line presents only the CCD series (CCD, 1.9 $M_\odot$), the dotted (orange) and dash-dotted (black) lines correspond to Gaia DR2 2018 data [12] and Tokovinin radial velocities [27] (G18T, 1.5 $M_\odot$) and Gaia DR2 [12] (G18G, 1.3 $M_\odot$). (d) Coincident AMP orbits obtained from different bases, corresponding to the sum of the component masses 1.7 $M_\odot$. See designations above.

1996 corresponding to $\beta < 0$ (see Table 6) and the orientation parameters (see Table 8).

Figure 5a shows about 300 positional observations of ADS 12169 according to the WDS catalog, including observations by W. Struve and the USNO observatory in Washington. It is obvious that Struve's first observations in 1819–1823 cannot be used to select the best orbit. Figure 5b present Pulkovo and space observations, as well as the ephemeris of Hale's orbit [6] and three AMP orbits from the 1996 family [15]. Moreover, the AMP orbit corresponding to $\beta = 0$ is in poor agreement with old observations. Figure 5c shows the ephemeris of new AMP orbits. Figure 5d presents, in addition to the new AMP orbits, the Hale orbit with $M_{AB} = 3.5 M_\odot$ c and the average Izmailov orbits without weights and with weights, the corresponding sums of the component masses are 25 and 16 $M_\odot$ (Table 7).

6. CONCLUSIONS

In this paper, we propose a modification of the AMP method: the coincidence of the orbits obtained from different bases leads to a single-valued orbit and the sum of the component masses.

The orbits of four visual binaries of the Pulkovo Research Program (ADS 246, 2757, 10386, and 12169) have been improved. A solution was obtained that is unambiguous in the sense of the certainty of the ascending node: orbits with periods of 1226, 1075, 4500, and 4900 years, the orientation of the orbits and the masses of these systems (0.59 ± 0.05, 1.7 ± 0.3,

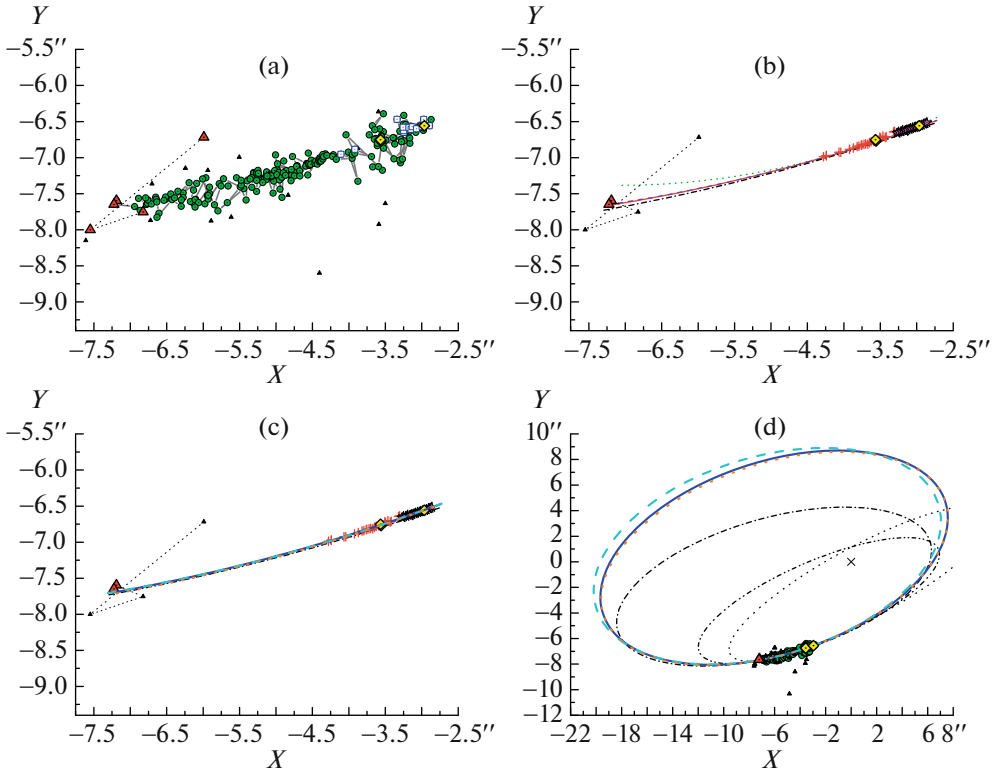

Fig. 5. Comparison of the orbits with observations for ADS 12169. (a) Observations according to the WDS catalog. The designations: the circles—the observations from WDS [11], the triangles—W. Struve's observations in 1819–1836 [11], the squares are photographic (for 1968 and 1976 [11]) and speckle interferometric (for 2000–2014 [11]) observations of the US Naval Observatory. Obviously, the last series is unreliable for control or selection of the best solution, and Struve's observations before 1832 cannot be used. (b) Pulkovo observations and preliminary orbits in 1994 and 1996. The crosses and asterisks show series of photographic [21] and CCD observations (Table 2) performed at the Pulkovo 26-inch refractor, the diamonds indicate Hipparcos space-born (1991) [11] and Gaia DR2 observations (2015) [12]; the dash-dotted black line shows the ephemeris for 1832–2025 orbits by Hale [6] (Table 7), the dotted, solid, and dashed lines are the ephemerides of the AMP orbits of the 1996 family [15], corresponding to $\beta = 0$, $\beta > 0$, and $\beta < 0$, the latter two practically coincide and describe the observations better, as well as Hale's orbit. (c) New AMP orbits. The solid, dashed, and dotted lines are AMP orbits obtained from the PCCD, CCD, and G18T ($\beta < 0$) bases, coinciding at 2.25 $M_\odot$. (d) New AMP orbits and 1996 and 2019 orbits. The dotted line and the dashed line with a double dotted line are Izmailov's orbits without weights and with weights according to [9], the corresponding sums of the component masses are equal to 25 and 16 $M_\odot$ (Table 7).

1.7 ± 0.4, and 2.25 ± 0.5 $M_\odot$), which, within the error limits, agrees with the mass–luminosity relation, but does not agree with the results of Hale and Izmailov obtained by the Thiele–Innes method.

In the problem of determining the orbits of wide stellar pairs, ground-based observations do not lose their relevance. It is necessary to continue dense homogeneous CCD-series with the 26-inch refractor of Pulkovo.

ACKNOWLEDGMENTS

The study was carried out using the WDS [11] and Gaia DR2 [12] catalogs. The authors express their deep gratitude to its creators, as well as personally B.D. Mason for providing WDS data upon our request. The authors are sincerely grateful to all the observers of the 26-inch refractor of the CAO RAS, especially to the co-authors of catalogs [21–23]. The authors are also grateful to O.V. Kiyaeva for valuable comments and advices. We propose to continue observations and studies of visual binaries of the Pulkovo program, including wide pairs with slow orbital motion, as well as work on the Pulkovo Catalog of Orbits of Wide Pairs.

FUNDING

This work was supported by a grant from the Russian Foundation for Basic Research (project 20-02-00563A).

REFERENCES

1. N. A. Shakht, L. G. Romanenko, D. L. Gorshanov, and O. O. Vasilkova, Solar Syst. Res. **50**, 56 (2016).
2. W. I. Hartkopf and B. D. Mason, *Sixth Catalog of Orbits of Visual Binary Stars* (US Naval Observatory, Washington, 2016). http://ad.usno.navy.mil/wds/orb6.html.

3. A. A. Kisselev and L. G. Romanenko, ASP Conf. Ser. **316**, 250 (2004).
4. J.-L. Agati, D. Bonneau, A. Jorissen, E. Soulie, S. Udry, P. Verhas, and J. Dommanget, Astron. Astrophys. **574**, A6 (2015).
5. W. I. Hartkopf, H. A. McAlister, and O. G. Franz, Astron. J. **98**, 1014 (1989).
6. A. Hale, Astron. J. **107**, 306 (1994).
7. B. D. Mason, W. I. Hartkopf, G. I. Wycoff, and E. R. Holdenried, Astron. J. **132**, 2219 (2006).
8. A. E. Baidin, N. I. Perov, and L. G. Romanenko, Vestn. SPbGU, Mat. Mekh. Astron., No. 5 (63), 154 (2018).
9. I. S. Izmailov, Astron. Lett. **45**, 30 (2019).
10. S. Blunt, E. L. Nielsen, R. J. de Rosa, Q. M. Konopasky, et al., Astron. J. **153**, 229 (2017).
11. B. D. Mason, G. L. Wycoff, and W. I. Hartkopf, *The Washington Visual Double Star Catalogue* (US Naval Observatory, Washington, 2018). http://ad.usno.navy.mil/wds/wds.html.
12. A. G. A. Brown, A. Vallenari, T. Prusti, J. H. J. de Bruijne, et al., Astron. Astrophys. **616**, A1 (2018).
13. A. E. Baidin, Cand. Sci. (Phys. Math.) Dissertation (Pulkovo Main Astron. Observ. RAS, St. Petersburg, Yaroslavl', 2018).
14. A. A. Kiselev and O. V. Kiyaeva, Sov. Astron. **24**, 708 (1980).
15. A. A. Kiselev and L. G. Romanenko, Astron. Rep. **40**, 795 (1996).
16. A. A. Kiselev, L. G. Romanenko, and O. A. Kalinichenko, Astron. Rep. **53**, 126 (1996).
17. O. V. Kiyaeva, L. G. Romanenko, and R. Ya. Zhuchkov, Astron. Lett. **43**, 316 (2017).
18. O. V. Kiyaeva and L. G. Romanenko, Astron. Lett. **46**, 555 (2020).
19. L. G. Romanenko and O. A. Kalinichenko, Astron. Astrophys. Trans. **31**, 7 (2019).
20. O. V. Kiyaeva, Sov. Astron. **27**, 701 (1983).
21. A. A. Kiselev, O. V. Kiyaeva, I. S. Izmailov, L. G. Romanenko, O. A. Kalinichenko, O. O. Vasil'kova, T. A. Vasil'eva, N. A. Shakht, D. L. Gorshanov, and E. A. Roschina, Astron. Rep. **58**, 78 (2014).
22. I. S. Izmailov, M. L. Khovricheva, M. Yu. Khovrichev, O. V. Kiyaeva, E. V. Khrutskaya, L. G. Romanenko, E. A. Grosheva, K. L. Maslennikov, and O. A. Kalinichenko, Astron. Lett. **36**, 349 (2010).
23. I. S. Izmailov and E. A. Roshchina, Astrophys. Bull. **71**, 225 (2016).
24. L. G. Romanenko, Astron. Rep. **61**, 206 (2017).
25. G. W. Marcy and K. J. Benitz, Astrophys. J. **344**, 441 (1989).
26. A. A. Tokovinin, A. Duquennoy, J.-L. Halbwachs, and M. Mayor, Astron. Astrophys. **282**, 831 (1994).
27. A. A. Tokovinin, Astron. Rep. **38**, 258 (1994).
28. J.-L. Halbwachs, M. Mayor, and S. Udry, Astron. Astrophys. **619**, A81 (2018).
29. L. G. Romanenko and A. A. Kiselev, Astron. Rep. **58**, 30 (2014).
30. A. A. Kiselev, L. G. Romanenko, I. S. Izmailov, and E. A. Grosheva, Izv. GAO at Pulkovo, **214**, 239 (2000).
31. S. L. Lippincott, Astron. J. **77**, 165 (1972).

Translated by E. Seifina